Polaron-ion correlations in Li_{x}FePO_{4} studied by x-ray nuclear resonant forward scattering at elevated pressure and temperature

S. J. Tracy, L. Mauger, H. J. Tan, J. A. Muñoz, Yuming Xiao, and B. Fultz

Phys. Rev. B **90**, 094303 — Published 12 September 2014

DOI: 10.1103/PhysRevB.90.094303

Polaron-ion correlations in Li_xFePO_4 studied by x-ray nuclear resonant forward scattering at elevated pressure and temperature

S. J. Tracy[1], L. Mauger[1], H. J. Tan[1], J. A. Muñoz[1], Y. M. Xiao[2] and B. Fultz[1]
[1] *W.M. Keck Laboratory, California Institute of Technology, Pasadena, California 91125, USA*
[2] *HPCAT, Geophysical Laboratory, Carnegie Institution of Washington, Argonne, Illinois 60439, USA*
(Dated: June 11, 2014)

Valence fluctuations of Fe^{2+} and Fe^{3+} were studied in a solid solution of Li_xFePO_4 by nuclear resonant forward scattering of synchrotron x-rays while the sample was heated in a diamond-anvil pressure cell. The spectra acquired at different temperatures and pressures were analyzed for the frequencies of valence changes using the Blume-Tjon model of a system with a fluctuating Hamiltonian. These frequencies were analyzed to obtain activation energies and an activation volume for polaron hopping. There was a large suppression of hopping frequency with pressure, giving an activation volume for polaron hopping of $5.8\pm0.7\,\text{Å}^3$. This large, positive value is typical of ion diffusion, which indicates correlated motions of polarons and Li^+ ions that alter the dynamics of both. Monte Carlo simulations were used to estimate the strength of the polaron-ion interaction energy.

PACS numbers: 72.20.Ee 71.38.-k 72.80.Sk 76.80.+y

I. INTRODUCTION

Lithium-iron phosphate, $LiFePO_4$, is a new material for cathode electrodes of rechargeable Li-ion batteries.[1] An important issue, however, is its low electrical conductivity; at low temperatures $LiFePO_4$ is an insulator with a band gap of approximately 3.7 eV.[2–4] $LiFePO_4$ has the orthorhombic olivine-type structure shown in Fig. 1. Layers of corner-sharing networks of canted FeO_6 octahedra in the b-c plane are spaced by phosphate tetrahedra. Li^+ cations form one-dimensional chains that run between the FeO_6 planes. Previous work showed that the Li^+ diffusion pathway is along these b-axis channels.[5,6] The electronic carrier mobility is expected to be two-dimensional, occurring within the layers of FeO_6 octahedra that are separated by insulating phosphate groups.

Experimental values of both electrical conductivity and Li^+ ion diffusivity in $LiFePO_4$ span several orders of magnitude.[7–13] These large discrepancies have been attributed to differences in samples and experimental technique.[14] It is generally accepted that Li^+ ion diffusivity is highly sensitive to defects in the one-dimensional channels along the b-axis. Less understood is the scatter in reported values of electrical conductivity, however, which contributed to an early controversy about whether the electronic conductivity can be improved by doping.[15] Measurements of bulk properties on polycrystalline samples also present challenges in decoupling the intrinsic conductivity from the interparticle conductivity. Nevertheless, a keen interest remains in improving the intrinsic electrical conductivity of $LiFePO_4$, and better understanding the transport of Li^+ ions and electrons.

As with many other transition metal oxides, the mechanism of electrical conductivity in mixed valent $Li_xFe^{2+}_xFe^{3+}_{1-x}PO_4$ is small polaron hopping.[16–18] A small polaron quasiparticle comprises an electron or hole localized by atomic displacements of neighboring anions. When an electron transfers between Fe^{2+} and Fe^{3+} sites, the local configurations of the FeO_6 octahedra must also transfer. The difference between these atomic configurations in $LiFePO_4$ is large. By removing Li^+ ions from the lattice, lithiated $Li_1Fe^{2+}PO_4$ is transformed into delithiated $Fe^{3+}PO_4$ with the same olivine-type structure. As the Fe ions change from Fe^{2+} to Fe^{3+} during delithiation, the average Fe-O bond lengths are reduced by 6%.[19]

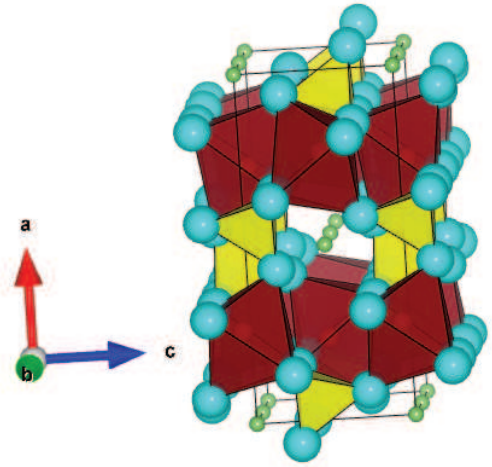

FIG. 1. (color online). Olivine-type structure of $LiFePO_4$ with chains of Li^+ ions (green), planes of FeO_6 octahedra (red) and phosphate tetrahedra (yellow).[20]

At moderate temperatures, the motion of a polaron quasiparticle is diffusive, and can be understood as an activated process with the jump rate[21,22]

$$\Gamma(T,P) \simeq \nu \exp(-2\alpha R) \exp\left(-\frac{E_a + PV_a}{k_B T}\right), \qquad (1)$$

where T is temperature, P is pressure, k_B is the Boltzmann constant, ν is a characteristic phonon frequency,

R is the Fe-Fe distance and α is the inverse localization length of the Fe wavefunctions. The activation energy, E_a, describes the energetic barrier for the polaron quasiparticle to transfer between adjacent iron sites. Previous measurements of bulk electronic conductivity as a function of temperature gave a wide range of activation energies between 155 and 630 meV.[15,23–26] Mössbauer spectrometry provides a more direct measurement of the rate of polaron hops between iron sites, and gives an activation energy around 500 meV.[16,17]

The effect of pressure on the activation barrier is quantified with an activation volume, V_a. PV_a is the extra enthalpy required from thermal fluctuations to induce a polaron hop when the material is under the pressure P. For $V_a > 0$, the activation barrier is effectively raised with pressure, and the polaron hopping frequency is suppressed. V_a is the difference in volume between the material with the configuration favorable for electron transfer, and the volume in the equilibrium configuration. It is expected to be local in origin, and is expected to reflect the local expansion or contraction in the vicinity of the hopping polaron. In accordance with the Frank-Condon principle, these local atomic distortions bring the electron levels of the initial and final states into coincidence, facilitating electron transfer. An understanding of V_a therefore gives insight into the atom configurations at the transient state of the polaron hop.

There have been few studies of the activation volume for polaron hopping. Previous measurements of electrical conductivity in geophysically-relevant oxides under applied pressure gave small, negative values for V_a of a few tenths of a cubic angstrom.[27–30] It has been suggested that the dominant effect in these systems was the decrease of R under pressure, allowing the electron to better sample the final state, therefore enhancing the polaron conductivity.[30] To our knowledge there has been no measurement of the electronic conductivity of $LiFePO_4$ under pressure.

Unlike the motion of polarons, the diffusion of Li^+ ions can be understood classically. Ion jumps into vacant neighboring sites occur by an activated process that does not sense the ion destination until after the jump is complete. First principles simulations suggest that Li^+ ions diffuse rapidly along a [010] channels, but there is a high energy barrier to cross between channels.[6] These calculations do not include defects or electron-ion interactions, however, and other reports suggest the material is a slow ion conductor.[7] The one dimensional character of the Li^+ mobility results in an ion conductivity that is highly sensitive to defects that block conduction channels, such as Li-Fe antisite point defects.[6,31]

Here we report new results on the charge dynamics at elevated pressure, obtained by performing measurements on Li_xFePO_4 heated in a diamond-anvil cell. The ^{57}Fe valence fluctuations in Li_xFePO_4 are strongly sensitive to pressure, giving a large and positive activation volume for polaron hopping that is more characteristic of ion diffusion. We show how this large effect could result from a correlated dynamics of polarons and mobile Li^+ ions. Previous density functional theory calculations for $LiFePO_4$ gave low activation barriers for polaron hopping compared to experimental results and this discrepancy was attributed to polaron-ion interactions.[32] The concept of a bound polaron has also been discussed in calculations of polaron migration barriers for lithium peroxide.[33] These studies assume a rigid lattice during electron transport, however. The authors state, "...the electron density alone is relaxed self-consistently and atom positions remain fixed for calculations along the migration path."[32] In other words, this method employs a linear combination of the initial and final states without allowing for ion rearrangements in the transition state, so $V_a = 0$. Ion-electron correlations have also been mentioned in reports of NMR and molecular dynamics studies on $LiMn_2O_4$ and Li_xNiO_2[34,35], for example, but there has been scant experimental evidence to support this concept. With a polaron-ion interaction, the activation enthalpy for moving a polaron depends in part on the ion motion by a vacancy mechanism. Vacancy diffusion is suppressed by pressure, and activation volumes for ion transport in oxides range from +1 to +10 Å^3.[36] Because ion transport is suppressed by pressure, polaronic conductivity should also be suppressed if the polaron-ion interaction energy, $E_{\rm pi}$, is large. In what follows, we estimate $E_{\rm pi}$ to be approximately –300 meV, which should have important consequences for the dynamics and positions of both polarons and ions.

II. EXPERIMENTAL

A solid solution of Li^+ ions in Li_xFePO_4 is stable at temperatures above 473 K, and is easily preserved at room temperature by quenching.[37,38] Previous x-ray diffractometry measurements showed that the olivine structures of $FePO_4$, $Li_{0.6}FePO_4$, and Li_1FePO_4 are stable to pressures of at least 30 GPa at 300 K.[39] Solid solutions of $Li_{0.6}FePO_4$ were prepared by a solid-state reaction and delithiated as described previously.[38,40] Powders were loaded into a Merrill-Bassett, Tel-Aviv-type, diamond-anvil cell[41] along with ruby chips for pressure measurement by the ruby florescence method.[42] The cells were prepared using rhenium gaskets and diamonds with 350 μm culets. The cell was heated in a resistive furnace with an Ar/1% H_2 atmosphere and kapton windows for x-ray transmission.

Nuclear forward scattering (NFS) measurements were performed at beamline 16ID-D at the Advanced Photon Source at Argonne National Laboratory. An avalanche photodiode detector was placed in the forward-scattered x-ray beam to measure transmitted intensity as a function of time. Four sets of measurements were taken at pressures of 0, 3.5, 7.1 and 17 GPa, with temperatures between 298 and 598 K. A high-resolution monochrometer tunes the incident beam to the 14.414 keV resonant energy and reduces the bandwidth to ∼2 meV. The syn-

chrotron flashes had durations of 70 ps, and were separated by 153 ns. Electronic scattering occurs within femtoseconds of the pulse arrival at the sample. The relatively long lifetime of the nuclear resonant state (τ=141 ns) allows for a clear separation of the prompt electronic scattering from the delayed, resonant scattering.

The ^{57}Fe nuclei in the sample are simultaneously excited by the synchrotron x-ray pulse, giving rise to coherent interference between emitted photons in the forward direction. When the degeneracy of the nuclear levels is lifted by hyperfine interactions, the phased de-excitation of slightly offset energy levels generates beat patterns in the transmitted intensity. Within the kinematical limit, the delayed emission in the forward direction is expressed as a sum over oscillatory terms whose arguments are the differences in the energies of the nuclear levels, superimposed on the exponential decay[43]

$$A(t) \sim \exp(-t/\tau) \sum_{j,l} \exp(-\mathrm{i}\omega_{j,l} t)\ \mathbf{a_0^*}\, W_j W_l\, \mathbf{a_0}\ . \quad (2)$$

Here W is the normalized weight of the nuclear transition, $\omega_{j,l} = \omega_j - \omega_l$ and $\mathbf{a_0}$ is the polarization unit vector of the synchrotron radiation. A sample with two Fe sites, each with a distinct value for quadrupole splitting (QS) and isomer shift (IS), will have 6 component beat frequencies in the transmitted intensity, each with a period that is inversely related to the difference in nuclear energy levels.

Nuclear resonant scattering allows for the study of local electron dynamics at iron ions. The measured spectra are altered when the hyperfine fields fluctuate on the same time scale as the characteristic frequency of the hyperfine interaction energies, $\hbar\omega$. In Li_xFePO_4 the frequency of valence fluctuations, and how this frequency changes with temperature, leads to rich variations of the shape and symmetry of the quadrupole doublets from Fe^{2+} and Fe^{3+}. At low frequencies and low temperatures, the spectral components from Fe^{2+} and Fe^{3+} remain distinct, and at very high frequencies the spectrum is a single doublet. The rich behavior occurs when the valence of a ^{57}Fe ion fluctuates between Fe^{2+} and Fe^{3+} at a frequency between 1 and 100 MHz. In conventional Mössbauer energy spectra the quadrupole doublets from Fe^{2+} and Fe^{3+} merge together, with asymmetric, non-Lorentzian lineshapes for these intermediate frequencies. For nuclear forward scattering (NFS) in the time domain, these effects are seen as a distortion and washing-out of the quantum beat pattern from interference of the nuclear hyperfine levels. Previous conventional Mössbauer energy spectrometry studies on Li_xFePO_4 reported dramatic spectral distortions at temperatures between 373 and 513 K.[16,17]

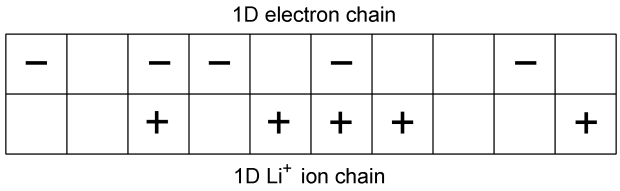

FIG. 2. Schematic of randomly populated 1D coupled Li^+ ion and electron chains.

III. SIMULATIONAL

The hops of electron-polarons are likely confined to the b-c plane, but they would tend to follow the one-dimensional paths of ions if the interactions between polarons and ions are strong. We performed a series of Monte Carlo (MC) simulations on a coupled pair of one-dimensional chains. As shown in Fig. 2, one chain contained Li^+ ions, and the other contained electron-polarons. The goal of these simulations was to estimate the strength of the polaron-ion interaction by comparing the simulated electron dynamics under pressure to the valence fluctuations measured by nuclear resonant scattering.

The hop of a Li^+ ion requires an empty site at an adjacent position on the ion chain, so ion diffusion was assumed to occur by a vacancy mechanism. Likewise, an electron-polaron at an Fe^{2+} site requires a neighboring Fe^{3+} on the same chain for the electron to hop, so a vacancy mechanism was used for the electron dynamics as well. Activated state rate theory was used to calculate jump probabilities of the ions and electrons (details are in the Appendix). The activation barrier for the ion depended only on the initial configuration of the ion, but in the adiabatic approximation the electron samples the initial and final state energies before making a transition.

For the results shown below, activation barriers were set using previous computational results for the "free-polaron" activation energy, E_p = 215 meV, and the activation energy for Li^+ ion diffusion, E_i = 270 meV[6,32] (although many other values were tried). These activation barriers were altered by a polaron-ion interaction energy, E_pi, the strength of the coupling between the Li^+ ion and the electron-polaron when the two are first nearest neighbors (1NN), being at the same sites on their respective chains. First principles calculations place E_pi in the range of –370 meV to –500 meV, depending on the degree of lithiation, and the authors suggested that the E_pi could affect polaron dynamics.[32] When a Li^+ ion jumps away from a 1NN electron, the activation barrier for the jump is raised by an amount $|E_\mathrm{pi}|$. The quantum character of the electrons gives an activation barrier that depends on the 1NN on the Li^+ chain in both the initial and final positions. Accordingly, the electronic activation barrier is raised by an amount $|E_\mathrm{pi}|$ when the electron jumps away from a Li^+ 1NN, and is lowered by an amount $|E_\mathrm{pi}|$ for a jump into a site with a Li^+ 1NN.

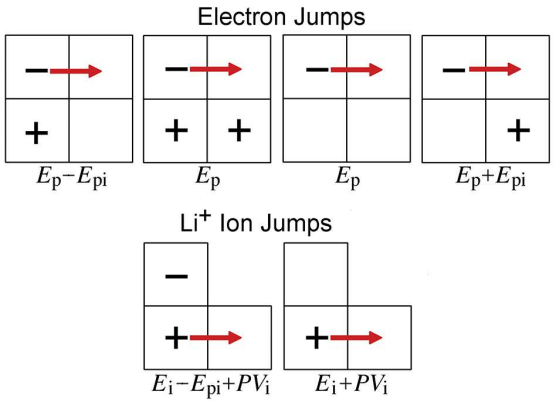

FIG. 3. Six subprocess describing ion and electron jumps on coupled 1D chains, where the energy barrier for each subprocess is listed below the schematic. E_p and E_i are the free polaron and ion activation barriers respectively, E_{pi} is the polaron-ion interaction energy, and V_i is the activation volume for ion hopping. For Li^+ ion jumps, depicted in the lower frames, the energy barrier depends only on the initial 1NN electron site; the final 1NN site on the electron chain is not depicted.

The possible jumps are broken down into the six subprocesses shown in Fig. 3.

The activation barrier for ion hopping was altered by an amount PV_i, where V_i is the activation volume for ion diffusion. An activation volume of +5 Å^3 was used, typical of activation volumes measured for ion diffusion in similar systems.[36] Assuming $LiFePO_4$ behaves similarly to other transition metal oxides, we expect the activation enthalpy for the hop of a bare electron-polaron to decrease with pressure.[27–30] Because this effect is expected to be an order of magnitude smaller than the effect on ionic diffusion, for the purpose of these simulations we treated the activation barrier for electron hopping as pressure independent.

IV. RESULTS

A. Experimental Results

The NFS spectra are presented in Fig. 4. In the 0 GPa series, with increasing temperature, especially above 400 K, the quantum beats are broadened and flattened, and the integrated count rate decreases. This washing out of the spectral features and suppression of count rate comes from a dephasing of the scattered intensity, consistent with the development of broad, asymmetric energy spectra. The temperature range of the onset of these effects is consistent with the polaron dynamics reported by conventional Mössbauer spectrometry.[17] At elevated pressures these large spectral distortions do not occur until higher temperatures, approximately 100 K higher for 3.5 GPa. Smaller changes can be seen at lower temperatures, however.

The spectra were evaluated using the software package CONUSS.[44,45] CONUSS allows for the calculation and refinement of spectra using the theory of Blume and Tjon for random temporal fluctuations of the hyperfine field.[46,47] Drawing on the Kubo-Anderson model of motional narrowing[48], Blume and Tjon used a correlation function, time averaged over the stochastic degrees of freedom, to evaluate the lineshapes of emitted radiation from a system with a fluctuating nuclear Hamiltonian. Depending on the relaxation time relative to the lifetime of the excited state, the effective widths of the resonance lines can either sharpen or broaden inhomogeneously and amalgamate. While the probability for a transition between the excited state and the ground state with the emission of photon is Lorentzian in form, the observed probability results from a sum over the possible ground states and a stochastic average over the sampled excited states. For polycrystalline samples, the problem reduces to the simplest case treated by Blume and Tjon in which the stochastic and quantum mechanical parts of the problem are separable as there is no issue of noncommutativity of the Hamiltonian at different times.

The fluctuations from polaron hopping require two sets of hyperfine parameters for the Fe^{2+} and Fe^{3+} sites, together with a relaxation matrix of transition rates, describing the random jumps between the two sets of hyperfine parameters

$$\mathbf{W} = \begin{bmatrix} -\Gamma\rho_{2+} & \Gamma\rho_{2+} \\ \Gamma\rho_{3+} & -\Gamma\rho_{3+} \end{bmatrix} . \tag{3}$$

The elements of the relaxation matrix are weighted by the populations, ρ, of the two sites, maintaining charge balance. This allows for the refinement of a QS specific to each site, a relative IS and a polaron hopping frequency, $\Gamma(T, P)$.

The Blume-Tjon model was not used for the spectra at 298 K. These spectra were fit with a static model, allowing for the refinement of the sample thickness as well as the distribution of QS that may result from disorder in the sample and pressure gradients in the cell. The sample thickness and the distribution of QS were then fixed for the fits at elevated temperatures, minimizing problems from correlations between the hopping frequency and the distribution of quadrupole splittings (which produce similar effects at low hopping frequencies). For fitting a data set at a fixed pressure, after fixing the thickness and the distribution of the QS at their values for 298 K, four parameters were varied to fit the spectra at elevated temperatures. The refined fits overlay experimental spectra in Fig. 4. Most of the hyperfine parameters showed gradual changes with temperature and pressure that we summarize here with linear relationships

QS of Fe^{2+}: $[2.9 - 2\times10^{-3}(T - 298)]$ mm(s K)$^{-1}$,
QS of Fe^{3+}: $[1.1 - 2\times10^{-3}(T - 298)]$ mm(s K)$^{-1}$,
Relative IS: $[0.8 - 10^{-3}(T - 298)]$ mm(s K)$^{-1}$,
QS of Fe^{2+}: $[2.9 + 0.04P]$ mm(s GPa)$^{-1}$,
QS of Fe^{3+}: $[1.1 + 0.04P]$ mm(s GPa)$^{-1}$.

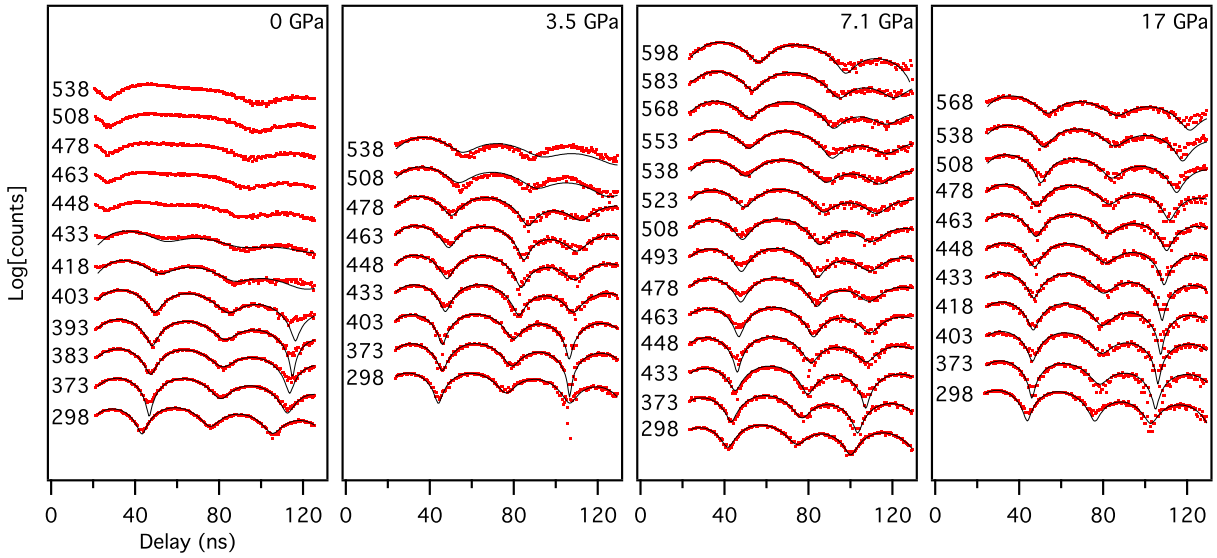

FIG. 4. (color online). Temperature series of NFS spectra taken at 0, 3.5, 7.1 and 17 GPa. The fits (black curves) overlay experimental data (red points). Temperatures are listed to left of spectra in Kelvin. The x-axis is the delay in nanoseconds after the arrival of the synchrotron pulse. The spectra have been scaled by their maximum value and offset for comparison.

The relative IS ($\mathrm{IS\,Fe^{2+}} - \mathrm{IS\,Fe^{3+}}$) did not show a discernible trend with pressure. These parameters are consistent with those determined using conventional conventional Mössbauer spectrometry for the same material.[16,17] The data and fits in Fig. 4 are plotted on a logarithmic scale. The fitting algorithm uses a least squares criterion, so the fit discrepancies in the regions of lowest count rate (most notably the third minima) are smaller than they appear and do not significantly affect the quality of the fits.

Figure 5(a) shows the polaron hopping frequencies, $\Gamma(T,P)$, determined from the fits to the spectra of Fig. 4. For frequencies below approximately 1 MHz, the spectra are fit equally well with a static model. In this low-frequency limit, a static spectrum and a dynamic spectrum are identical, all else held constant. For the 17 GPa series, the hopping frequencies for the entire temperature series were below this threshold. The suppression of hopping frequencies at moderate pressures indicates that V_a is positive and large. The three data sets in Fig. 5(a) were fit simultaneously with Eq. 1 to determine the activation enthalpies and the prefactor. From the ambient pressure series, the activation energy was found to be 470±50 meV, where the uncertainty arises from the weighting of the different data points in linear or logarithmic fits, and the choice a prefactor for Eq. 1. This is comparable to the values of 512, 550, and 570 meV for activation energies of hyperfine parameters from the same material measured by conventional Mössbauer spectrometry.[16]

The prefactor was first assumed independent of pressure. The result, $\sim 10^{13}$ Hz, is typical of optical phonon frequencies measured by inelastic neutron scattering and by Raman spectrometry.[49,50] For a second set of fits, we calculated the pressure dependence of the prefactor, $\nu \exp(-2\alpha R)$. We extrapolated the attempt frequency to elevated pressure using a typical Grüneisen parameter, $\gamma = 2$, and the compressibility, κ_T,

$$\nu(P) \simeq \nu_0(1 + \gamma P \kappa_T) \; . \tag{4}$$

The wavefunction overlap was approximated assuming a pressure independent localization length

$$\exp[-2\alpha R] \simeq \exp[-2\alpha R_0(1 - P\kappa_T/3)] \; , \tag{5}$$

where R_0 is the ambient pressure inter-cation distance. X-ray diffractometry measurements at 300 K on an olivine $Li_{0.6}FePO_4$ solid solution at pressures up to 32 GPa gave a bulk modulus of 120±4 GPa.[39] This is somewhat larger than for Li_1FePO_4, with bulk modulus measured as 106±8 GPa, and calculated as 96 GPa.[51] These additional considerations did not significantly affect the results below for V_a.

From Eqs. 1, 4 and 5, V_a can be determined from the pressure dependence of the activation enthalpy. For a given pressure, we determine the activation enthalpy by looking at the linear part of $\ln(\Gamma)$ as a function of β, where $\beta = 1/(k_B T)$.[28]

$$\ln(\Gamma) = -\beta \Delta H - 2\alpha R + \ln(\nu) \; , \tag{6}$$

$$\Delta H \simeq -\left(\frac{\partial \ln(\Gamma)}{\partial \beta}\right)_P \; . \tag{7}$$

To account for any pressure dependence of the prefactor of Eq. 1, we consider the pressure dependence of the last

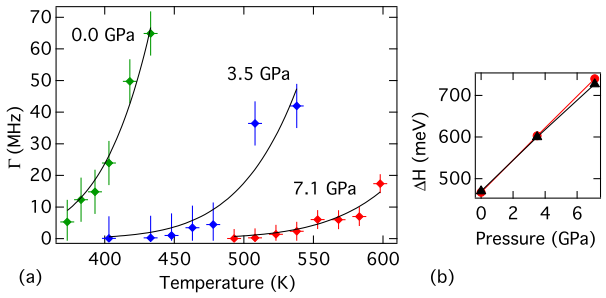

FIG. 5. (color online). (**a**) Polaron hopping frequencies, $\Gamma(T,P)$, at 0, 3.5 and 7.1 GPa, as determined from the solid curves of Fig. 4. Solid curves are Arrhenius-type fits using a pressure-independent prefactor. (**b**) Activation enthalpies, $\Delta H = E_a + PV_a$, versus pressure, where $E_a = 470$ meV. Black triangles are results for fixed prefactor, red circles are for a pressure dependent prefactor.

two terms in Eq. 6. Assuming these terms are independent of temperature, Eqs. 4 and 5 can be used to correct the V_a obtained from the jump rates, $\Gamma(T,P)$,

$$V_a = \left(\frac{\partial \Delta H}{\partial P}\right) , \tag{8}$$

$$V_a \approx -\frac{\partial \left(\frac{\partial \ln \Gamma}{\partial \beta}\right)_P}{\partial P} + \frac{2\,\alpha R_0\,\kappa_T}{3\,\beta} + \frac{\gamma \kappa_T}{\beta} . \tag{9}$$

The dominant source of error in the determination of the enthalpies lies in the choice of a prefactor for Eq. 1. Constraining the prefactor to a reasonable range based on past measurements of optical phonons[49,50,52] gives an error in the magnitude of the activation enthalpies of approximately ±10%. The slope of the curve in Fig. 5(b) gives an activation volume of $+5.8 \pm 0.7$ Å^3. The second and third terms of Eq. 9 are an order of magnitude smaller than the first term from the slope of Fig. 5(b), but will increase V_a above the value of +5.8 Å^3. Our V_a is between 1 and 2 orders of magnitude larger than previously reported polaron activation volumes from resistivity measurements on oxides.[27–30]

B. Simulational Results

Polaron jump frequencies were calculated as a function of pressure, assuming these frequencies were proportional to Boltzmann factors with thermal activations. The activation energies were taken as the appropriate combinations of E_p, E_i, and E_{pi}, depending on their local configurations. The activation energy for an ion jump was increased with pressure by PV_i, where V_i was +5 Å^3 and P was 0, 3 or 7 GPa. We used values of $E_p = 215$ meV and $E_i = 270$ meV as reported in literature[6,32], but we also calculated frequencies using several other activation barriers ranging from 50% to 200% of these values.

For simulations with $|E_{pi}|$ greater than 100 meV, after a quick initial relaxation, more than 90% of the electrons were paired to a Li^+ across the coupled chains. By inspecting the jump probabilities of Eqs. A8 – A11, we found that E_{pi}=–300 meV could account for the experimental trend in the pressure-induced suppression of the polaron jump frequency at $T = 573$ K. Nevertheless, values of E_{pi} from –200 to over –400 meV gave similar results.

In the MC simulations, we monitored the mean-squared displacement (MSD) of both species as a function of pressure and E_{pi}. Our interest was how the electron MSD was altered under pressure as a result of suppressed ionic mobility. The simulations varied the ionic mobility while monitoring the effect on the electronic mobility. The activation barrier for electron hopping was pressure independent, so raising the activation barrier for ion hopping (through pressure) has no effect on the electron MSD when the ion and electron chains are decoupled (E_{pi}=0). When a coupling is introduced, an indirect effect on the electron mobility is observed with increasing $|E_{pi}|$. Fig. 6 presents typical results of such a series of simulations. The electron MSD increases approximately as $t^{0.5}$. This exponent is well-known when particles cannot pass on a 1D chain and require concentration fluctuations to move forward.[53] A suppression of the MSD with pressure clearly emerges for values of E_{pi} less than –200 meV and becomes increasingly pronounced as the magnitude of E_{pi} is increased. For a polaron-ion interaction energy of –250 meV at 3 GPa the MSD is suppressed by 45% and at 7 GPa the MSD is suppressed an additional 40%. For agreement with experiment, it appears that E_{pi} for $LiFePO_4$ is between –200 and –300 meV. Larger magnitude values are not ruled out, however. The effects of pressure on the polaron jump frequency saturated when $|E_{pi}|$ was somewhat larger than E_p. It was also noted that the effects of pressure on the polaron jump rate became larger as E_i decreased relative to E_p, consistent with a larger role of ion motion in the overall dynamics.

V. DISCUSSION

Holstein's molecular crystal model captures the essential physics of small polaron formation and dynamics.[54–56] A tight-binding model is used to describe an extra electron in an array of N molecules, each with an internuclear distortion variable, x_n, and a reduced mass M, where $M^{-1} = N^{-1} \sum_{\text{ions}} m^{-1}$. The positive strain energy is quadratic in the x_n (e.g., the interatomic separation of two ions in a diatomic molecule) with harmonic oscillator frequency, ω_0, associated with the configurational coordinate of an isolated molecule. The electronic energy is reduced linearly with x_n in proportion to the strength of an electron-phonon interaction parameter, A, that characterizes the electron-lattice coupling strength in units of force.

A finite local distortion, x_n, results in a reduced po-

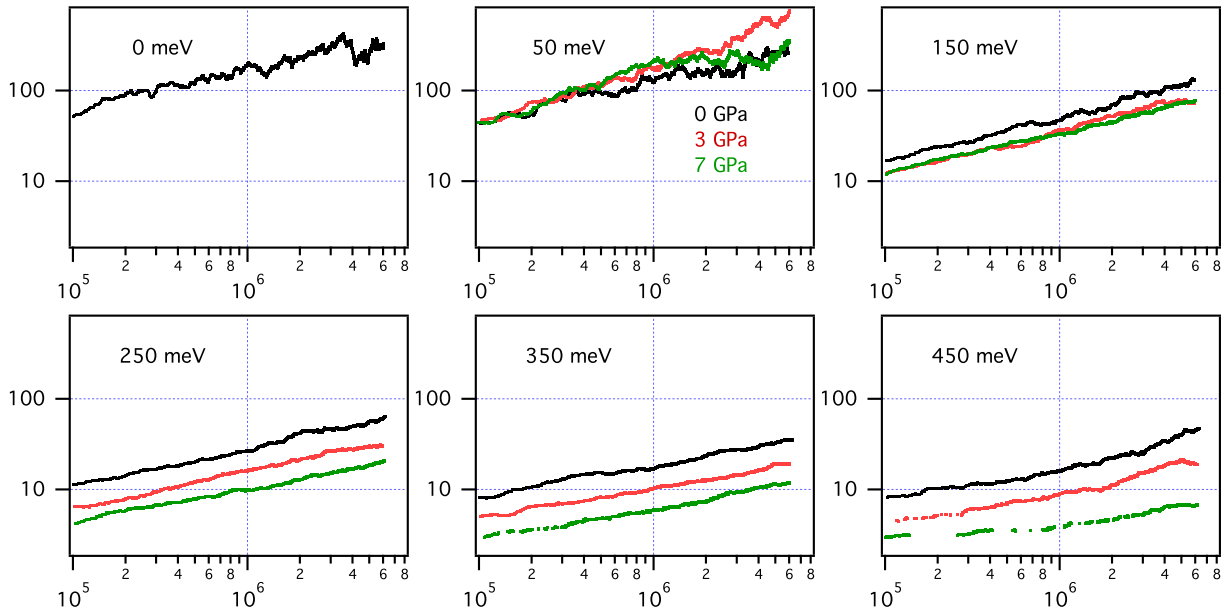

FIG. 6. (color online). Electron MSD versus time for six series of MC-simulations for a pair of coupled 1D ion and electron chains. (Units for MSD are site index. Time is dimensionless.) Each subplot shows the results for a different $E_{\rm pi}$. Subplots are labeled with -$E_{\rm pi}$ (0, 50, 150, 250, 350 and 450 meV). In each series, the MSD is shown for three different pressures: 0 (black), 3 (red) and 7 GPa (green).

tential that effectively pins the electron, so the localized polaron is favored by the binding energy, E_b, relative to an electron in an undeformed lattice

$$E_b \approx \frac{A^2}{2M\omega_0^2} \,. \tag{10}$$

In the adiabatic limit, the prefactor in Eq. 1 reduces to the mean optical phonon frequency and the activation energy is lowered by an amount J, associated with the d-bandwidth,[27]

$$E_a = \frac{E_b}{2} - J \,. \tag{11}$$

The activation energy depends on pressure through the exchange integral, J, as well as any pressure dependence of the binding energy. Taking the activation volume as the pressure derivative of the activation energy,

$$V_a = \frac{\partial E_a}{\partial P} \approx E_b \left(\frac{1}{A}\frac{\partial A}{\partial P} - \frac{1}{\omega_0}\frac{\partial \omega_0}{\partial P} \right) - \frac{\partial J}{\partial P} \tag{12}$$

and using the definition of the compressibility and the Grüneisen parameter, γ, the activation volume becomes,

$$V_a \approx E_b \left(\frac{1}{A}\frac{\partial A}{\partial P} - \gamma\kappa_T \right) - \frac{\partial J}{\partial P} \,. \tag{13}$$

The last term, from the increased wavefunction overlap, is positive, and tends to destabilize the localized polaron. This term is believed to be responsible for the negative activation volumes in other polaronic conductors.[27] Our large, positive V_a would be consistent with an effect of pressure on the electron-phonon interaction parameter, A, if $\partial A/\partial P > 0$, giving $\partial E_b/\partial P > 0$ by Eq. 10. In general, however, we expect destabilization of an electron polaron centered at a Fe^{2+} ion because the compressibility of ferrous-oxygen bonds is greater than for ferric-oxygen bonds. First principles calculations suggest the activation barrier is raised by ~50 meV under 4% biaxial compression (along the b and c axes).[57] The authors attribute this effect to an enhancement of the electron-phonon coupling. Frozen phonon calculations for the strained system show the electron phonon coupling constant increases by more than 20%.[57] These effects on the activation barrier from standard polaron models are too small, or of the wrong sign, to account for our experimental results.

The electron-phonon interaction could be affected by the electrostatic interaction between the polaron and a nearby Li^+ ion if the ion has a pressure-dependent mobility. We suggest the origin of our large difference between the activation volume measured for $LiFePO_4$ and previous activation volumes determined using conductivity measurements on oxides without mobile ions is the strong coupling between the polarons and the mobile Li^+ ions, $E_{\rm pi}$.

Previous first principles calculations for polaron hopping in $LiFePO_4$ gave activation energies of 175 and 215 meV for electron and hole polarons, respectively.[32] These results are for free-polaron transport. Measured activation energies, from either Mössbauer spectrometry or conductivity measurements, are two to three times higher

than these calculated values. This is consistent with a tendency for the electrons on Fe^{2+} sites to remain near Li^+ ions.

The effect of pressure on valence fluctuations at Fe sites is indirect, but potentially large. It is well known that pressure suppresses ionic diffusion by a vacancy mechanism (as in Eqs. A4 and A5). The MC simulations show how polaron dynamics are suppressed if the polaron-ion interaction energy tends to attract the polaron to immobile ions. The required interaction energy, $E_{\rm pi}$, is approximately –300 meV for the pressures and temperatures of interest.

Some discrepancies deserve further investigation. Electron jumps between two sites where both have ion neighbors, or both have vacancies (middle processes at top of Fig. 3), are unaffected by pressure, and predict a background dynamics that is not found experimentally. In the olivine structure, electron mobility is likely confined to the b-c plane. The Fe and Li sites are staggered in a way that each Fe site has two symmetrically positioned Li sites, but within a given FeO_6 plane each Li-site has one 1NN Fe site and one second-nearest-neighbor (2NN) Fe site. A polaron following the path of closest approach to a given ion chain will necessarily alternate between these 1NN and 2NN-type sites where the Li-Fe bond length is 6% longer in the 2NN site.[19] When pressure immobilizes the Li^+ ions, there may be a tendency for electron-polarons to localize in these 1NN-type sites in such a way that local dynamics are suppressed. Alternatively, the experimental technique may not be sensitive to certain dynamics, for example minority processes or dynamics that fall outside the window of sensitivity of frequencies sampled by Mössbauer spectrometry measurements. It is also possible that pressure suppresses other aspects of polaron dynamics, or the ions and polarons may form an ordered structure with reduced dynamics.

The generally good agreement between the experiment and simulated dynamics with a reasonable value of $E_{\rm pi}$, together with a measured activation volume of +5.8 Å^3, consistent with ion diffusion, indicate a strong coupling between the ions and polarons in Li_xFePO_4. A transport of net charge requires decoupling of the ion and polaron motions, however, so the coupling is not immutable. Nevertheless, the correlated motions of electrons and ions should suppress electrical conductivity in $LiFePO_4$. Furthermore, a large correlation in the motions of polarons and ions can explain why the electrical conductivity of $LiFePO_4$ is so sensitive to materials preparation. Because Li^+ diffusion in $LiFePO_4$ is essentially one dimensional, Li^+ ion mobility suffers as a result of channel blockage by defects.[6,31] Blocked channels for Li^+ ions then suppress electronic conductivity if polaron-ion interactions are strong. This effect may be common in materials when both ions and electrons are mobile.

A small polaron quasiparticle comprises an electron localized by atomic contractions from neighboring anions. Both the charge and distortion of the polaron are large enough to interact with the charge and distortion around a Li^+ ion, altering the formation energy and dynamics of the polaron. The quantum dynamics of small polaron hopping is likely modified by the classical dynamics of ion motion; likewise, the configurations of polarons and ions on the crystal lattice should also be affected by these interactions.

VI. CONCLUSIONS

Nuclear resonant scattering spectra of Li_xFePO_4 were measured at elevated pressure and temperature. An analysis of the spectra using the Blume–Tjon model for a system with a fluctuating electric field gradient gave frequencies of Fe valence fluctuations that correspond to frequencies of polaron hopping. From measurements over a range of temperatures and pressures, both the activation energy and activation volume were determined for polaron hopping. To our knowledge this is the first measurement of an activation volume for polarons in a material with mixed ion-polaron conductivity.

Pressure caused a large suppression of valence fluctuations in Li_xFePO_4, giving an activation volume for polaron hopping of +5.8 Å^3. This unusually large and positive activation volume is not typical of bare polaron hopping. It indicates a correlated motion of polarons and Li^+ ions. From model calculations and Monte Carlo simulations, the binding energy between the polaron and the Li^+ ion was found to be approximately –300 meV. This strong binding and polaron-ion correlation should suppress the intrinsic electronic conductivity of Li_xFePO_4. It may also affect the diffusion of Li^+ ions. Such coupled processes may be common to other materials where both ions and polarons are mobile.

ACKNOWLEDGMENTS

We thank C. W. Li for discussions. Portions of this work were performed at HPCAT (Sector 16), Advanced Photon Source (APS), Argonne National Laboratory. HPCAT is supported by CIW, CDAC, UNLV and LLNL through funding from DOE-NNSA, DOE-BES and NSF. Use of the APS was supported by DOE-BES, under Contract No. DE-AC02-06CH11357. This work was supported as part of EFree, an Energy Frontier Research Center, under Award No. DE-SG0001057.

Appendix A: Monte Carlo Algorithm

Each chain depicted in Fig. 2 had 3000 sites and periodic boundaries. Half of the sites on each chain were initially populated at random, one with Li^+ ions, and the other chain with electrons. Both species moved along their respective chains by a vacancy-type mechanism. For each step in the simulation, every site on both chains was selected in a random sequence. If the site contained

an electron or ion, the probability that a jump will occur was calculated using Boltzmann factors, described below, for $T = 573$ K. The time was obtained as a running sum of the inverse of the Boltzmann factors of the jumps that occurred.

The energies used in the Boltzmann factors are

$$\{E_{\rm i},\ E_{\rm p},\ E_{\rm pi}\}\ , \tag{A1}$$

where the first two are activation energies for the jump of a bare (noninteracting) ion and a polaron, respectively, and the third is the polaron-ion interaction energy. For a given event, the relevent site occupancies of the electron or ion on a site were either 0 or 1, as set by four Kroneker δ-functions. For a site directly opposite on the other chain the index is 0, to its left –1, or right +1

$$\{\delta_{0\rm p},\ \delta_{0\rm i},\ \delta_{-1\rm i},\ \delta_{+1\rm i}\}\ . \tag{A2}$$

The two Kroneker δ-functions for the vacancy pertain to vacancies on the same chain as the moving species, which allow the jump to occur to the left or right (±1)

$$\{\delta_{-1\rm v},\ \delta_{+1\rm v}\}\ . \tag{A3}$$

The Boltzmann factors for the four jumps to the left or right by the ion or electron-polaron are

$$B_{-1\rm i} = \delta_{-1\rm v}\exp\Big(-\beta(E_{\rm i}+PV_{\rm i}+\delta_{0\rm p}E_{\rm pi})\Big)\ , \tag{A4}$$

$$B_{+1\rm i} = \delta_{+1\rm v}\exp\Big(-\beta(E_{\rm i}+PV_{\rm i}+\delta_{0\rm p}E_{\rm pi})\Big)\ , \tag{A5}$$

$$B_{-1\rm p} = \delta_{-1\rm v}\exp\Big(-\beta[E_{\rm p}+(\delta_{0\rm i}-\delta_{-1\rm i})E_{\rm pi}]\Big)\ , \tag{A6}$$

$$B_{+1\rm p} = \delta_{+1\rm v}\exp\Big(-\beta[E_{\rm p}+(\delta_{0\rm i}-\delta_{+1\rm i})E_{\rm pi}]\Big)\ , \tag{A7}$$

where the ion jump is influenced by pressure, and depends on the presence of an electron-polaron directly opposite (subscript 0), whereas the electron jump depends on the presence of an ion directly opposite, but also opposite from its final position after the jump.

The jump probabilities were normalized by the two possibilities that could occur and the possibility of no event

$$\Gamma_{-1\rm i} = \frac{B_{-1\rm i}}{1+B_{-1\rm i}+B_{+1\rm i}}\ , \tag{A8}$$

$$\Gamma_{+1\rm i} = \frac{B_{+1\rm i}}{1+B_{-1\rm i}+B_{+1\rm i}}\ , \tag{A9}$$

$$\Gamma_{-1\rm p} = \frac{B_{-1\rm p}}{1+B_{-1\rm p}+B_{+1\rm p}}\ , \tag{A10}$$

$$\Gamma_{+1\rm p} = \frac{B_{+1\rm p}}{1+B_{-1\rm p}+B_{+1\rm p}}\ . \tag{A11}$$

At each step of the simulation, the state of the chains was used to obtain the Kroneker δ-functions needed for Eqs. A4 through A7. The electron or ion under consideration moved left, right or remained stationary based on a randomly generated number, Q, between 0 and 1. For a given electron, a left jump occurred when $Q < \Gamma_{-1\rm p}$, a right jump when $\Gamma_{-1\rm p} < Q < \Gamma_{+1\rm p}+\Gamma_{-1\rm p}$ and no jump when $Q > \Gamma_{+1\rm p}+\Gamma_{-1\rm p}$. Ion jumps were determined similarly. The local change after a successful jump was used to update the state of the chains, and the inverse of the Boltzmann factor was added to the time.

[1] A. K. Padhi, K. S. Nanjundaswamy, and J. B. Goodenough, J. Electrochem. Soc. **144**, 1188 (1997).
[2] F. Zhou, K. Kang, T. Maxisch, G. Ceder, and D. Morgan, Solid State Commun. **132**, 181 (2004).
[3] K. Zaghib, A. Mauger, J. B. Goodenough, F. Gendron, and C. M. Julien, Chem. Mater. **19**, 3740 (2007).
[4] M. K. Kinyanjui, P. Axmann, M. Wohlfahrt-Mehrens, P. Moreau, F. Boucher, and U. Kaiser, J. Phys. C: Solid State Phys. **22**, 275501 (2010).
[5] S.-i. Nishimura, G. Kobayashi, K. Ohoyama, R. Kanno, M. Yashima, and A. Yamada, Nat. Mater. **7**, 707 (2008).
[6] D. Morgan, A. Van der Ven, and G. Ceder, Electrochem. Solid St. **7**, A30 (2004).
[7] P. Prosini, M. Lisi, D. Zane, and M. Pasquali, Solid State Ionics **148**, 45 (2002).
[8] J. Sugiyama, H. Nozaki, M. Harada, K. Kamazawa, Y. Ikedo, Y. Miyake, O. Ofer, M. Mansson, E. J. Ansaldo, K. H. Chow, G. Kobayashi, and R. Kanno, Phys. Rev. B **85**, 054111 (2012).
[9] R. Amin, J. Maier, P. Balaya, D. P. Chen, and C. T. Lin, Solid State Ionics **179**, 1683 (2008).
[10] C. Delacourt, J. Rodriguez-Carvajal, B. Schmitt, J. Tarascon, and C. Masquelier, J. Electrochem. Soc. **7**, 1506 (2005).
[11] C. Zhu, K. Weichert, and J. Maier, Adv. Funct. Mater. **21**, 1917 (2011).
[12] R. Amin, P. Balaya, and J. Maier, Electrochem. Solid-State Lett. **10**, A13 (2007).
[13] M. Park, X. Zhang, M. Chung, G. B. Less, and A. M. Sastry, J. Power Sources **195**, 7904 (2010).
[14] R. Malik, A. Abdellahi, and G. Ceder, J. Electrochem. Soc. **160**, A3179 (2013).
[15] S.-Y. Chung, J. T. Bloking, and Y.-M. Chiang, Nat. Mater. **1**, 123 (2002).
[16] H. J. Tan, J. L. Dodd, and B. Fultz, J. Phys. Chem. C **113**, 2526 (2009).
[17] J. L. Dodd, I. Halevy, and B. Fultz, J. Phys. Chem. C **111**, 1563 (2007).
[18] B. Ellis, L. K. Perry, D. H. Ryan, and L. F. Nazar, J. Am. Chem. Soc. **128**, 11416 (2006).
[19] A. Andersson, B. Kalska, L. Haggstrom, and J. Thomas, Solid State Ionics **130**, 41 (2000).
[20] K. Momma and F. Izumi, J Appl. Crystallogr. **44**, 1272 (2011).
[21] N. Mott, J. Non-Cryst. Solids **1**, 1 (1968).
[22] I. Austin and N. Mott, Adv. Phys. **18**, 41 (1969).
[23] M. Takahashi, S. Tobishima, K. Takei, and Y. Sakurai, Solid State Ionics **148**, 283 (2002).
[24] S. Shi, L. Liu, C. Ouyang, D. Wang, Z. Wang, L. Chen, and X. Huang, Phys. Rev. B **68**, 195108 (2003).

[25] Y. Xu, S. Chung, J. Bloking, Y. Chiang, and W. Ching, Electrochem. Solid-State Lett. **7**, A131 (2004).

[26] C. Delacourt, L. Laffont, R. Bouchet, C. Wurm, J. Leriche, M. Morcrette, J. Tarascon, and C. Masquelier, J. Electrochem. Soc. **152**, A913 (2005).

[27] A. Goddat, J. Peyronneau, and J. P. Poirier, Phys. Chem. Miner. **27**, 81 (1999).

[28] T. J. Shankland, J. Peyronneau, and J. P. Poirier, Nature **366**, 453 (1993).

[29] D. P. Dobson and J. P. Brodholt, J. Geophys. Res. **105**, 531 (2000).

[30] J. Poirier, A. Goddat, and J. Peyronneau, Philos. Trans. R. Soc. London, Ser. A **354**, 1361 (1996).

[31] P. Axmann, C. Stinner, M. Wohlfahrt-Mehrens, A. Mauger, F. Gendron, and C. M. Julien, Chem. Mater. **21**, 1636 (2009).

[32] T. Maxisch, F. Zhou, and G. Ceder, Phys. Rev. B **73**, 104301 (2006).

[33] S. P. Ong, Y. Mo, and G. Ceder, Phys. Rev. B **85**, 081105 (2012).

[34] C. Chazel, M. Menetrier, L. Croguennec, and C. Delmas, Inorg. Chem. **45**, 1184 (2006).

[35] K. Tateishi, D. du Boulay, and N. Ishizawa, Appl. Phys. Lett. **84**, 529 (2004).

[36] G. A. Samara, Solid State Phys. **38**, 1 (1984).

[37] C. Delacourt, P. Poizot, J. Tarascon, and C. Masquelier, Nat. Mater. **4**, 254 (2005).

[38] J. L. Dodd, R. Yazami, and B. Fultz, Electrochem. Solid St. **9**, A151 (2006).

[39] J. L. Dodd, Ph.D. thesis, California Institute of Technology (2007), Appendix. `http://resolver.caltech.edu/CaltechETD:etd-05072007-184544`.

[40] K. Amine, J. Liu, and I. Belharouak, Electrochem. Commun. **7**, 669 (2005).

[41] E. Sterer, M. P. Pasternak, and R. D. Taylor, Rev. Sci. Instrum. **61**, 1117 (1990).

[42] A. Jayaraman, Rev. Mod. Phys. **55**, 65 (1983).

[43] W. Sturhahn, E. Alp, T. Toellner, P. Hession, M. Hu, and J. Sutter, Hyperfine Interact. **113**, 47 (1998).

[44] W. Sturhahn, Hyperfine Interact. **125**, 149 (2000).

[45] W. Sturhahn and E. Gerdau, Phys. Rev. B **49**, 9285 (1994).

[46] M. Blume and J. A. Tjon, Phys. Rev. **165**, 446 (1968).

[47] J. A. Tjon and M. Blume, Phys. Rev. **165**, 456 (1968).

[48] P. W. Anderson, J. Phys. Soc. Jpn. **9**, 316 (1954).

[49] R. Stevens, J. L. Dodd, M. G. Kresch, R. Yazami, B. Fultz, B. Ellis, and L. F. Nazar, J. Phys. Chem. B **110**, 22732 (2006).

[50] C. Burba and R. Frech, J. Electrochem. Soc. **151**, A1032 (2004).

[51] T. Maxisch and G. Ceder, Phys. Rev. B **73**, 174112 (2006).

[52] S. L. Shang, Y. Wang, Z. G. Mei, X. D. Hui, and Z. K. Liu, J. Mater. Chem. **22**, 1142 (2012).

[53] P. M. Richards, Phys. Rev. B **16**, 1393 (1977).

[54] T. Holstein, Ann. Phys. **8**, 325 (1959).

[55] T. Holstein, Ann. Phys. **8**, 343 (1959).

[56] D. Emin, Adv. Phys. **24**, 305 (1975).

[57] J. Lee, S. J. Pennycook, and S. T. Pantelides, Appl. Phys. Lett. **101** (2012).